Pure Ti fitting

Tigany Zarrouk

September 4, 2021

Contents

1   Fitting a titanium tight-binding model

1.1   Introduction (What, how, where, when, why?)

Fitted canonical d titanium model such that we could have a better description of titanium within a tight-binding framework. Empirical potential are not accurate enough to describe the intricacies of the titanium structure.

1.2   Fitting

The overlap integrals were chosen to have a simple exponential distance dependence, as initially formulated by Ducastelle, [?] and Allan [?]. This form was originally motivated by an approximation to the density of states, of which the form was taken to be a Gaussian fitted to the second-moment of the distribution [?]. Analysis of the hybridisation of d states with nearly-free electron states in transition metals gives rise to \$d\$-band resonances, which suggest a fifth-degree power law distance dependence of d-orbitals for the matrix elements [?, ?, ?, ?, ?]. However, it has not been shown that a power-law dependence exhibits better transerability over a simple exponential dependence [?, ?]. Many power-law models have not fared well in predicting data outside of their fitting range [?, ?, ?, ?, ?]. Furthermore, exponentials do not have large first or second derivatives compared to power laws when modified by the cutoff function, which complicates fitting for elastic properties,

and would provide erroneous forces [?]. Transferability has been consistently shown for the iron tight-binding model created by Paxton and Elsässer [?], which a more flexible exponential dependence. Their model predicts data well outside of their fitting range: non-degenerate dislocation core structures found in the bcc phase [?, ?], phonons and vacancy-formation energies. In addition, the Fe-Fe interactions have been shown suitable when incorporated with Fe-H/Fe-C interactions, to describe of hydrides and carbides [?, ?].

The bond integrals and pair potential ranges were chosen to start decaying to zero by a multiplicative polynomial between first and second neighbours in the hcp structure, going to zero between the second and third-neighbours. It was verified that the cutoffs were not close to neighbour shells found in titanium polymorphs, such that in future simulations, there would be no large and sudden forces arising from the inclusion of extra neighbours upon deformation. A multiplicative cutoff type was preferred over augmentative as it has been shown mitigate the effect of large second-derivatives, which would cause difficulty in replicating experimental elastic constants and phonon dispersion [?].

In fitting, it was found that having only first-neighbour interactions, did not give desirable properties for the hcp phase: elastic constants which resulted in negative Cauchy pressures and a poor description of the energy difference between titanium polymorphs. Increasing the range of the interactions to second-neighbours resulted in more favourable results.

The form of the pair potential was chosen to be simple sum of two exponentials and a rapidly decaying power law term. The exponentials, which have one large positive term, and a smaller negative term, contribute the most over the range of interaction, with the power law chosen to only increase the repulsion at smaller distances. The addition of this power law gave more desirable gamma surface energies more reminiscent of DFT. This will be discussed in section **SECTION LABEL**. The resultant pair potential was highly repulsive at short distances, yet became slightly attractive at larger distances. This allowed for one to approximately account for attractive effect of *sd* hybridisation in this simple d-orbital only model, as done in previous exclusively d-orbital tight-binding models for titanium [?]. Even though hybridisation is not strictly pairwise in character, we did not deem it necessary at this time to complicate matters further.
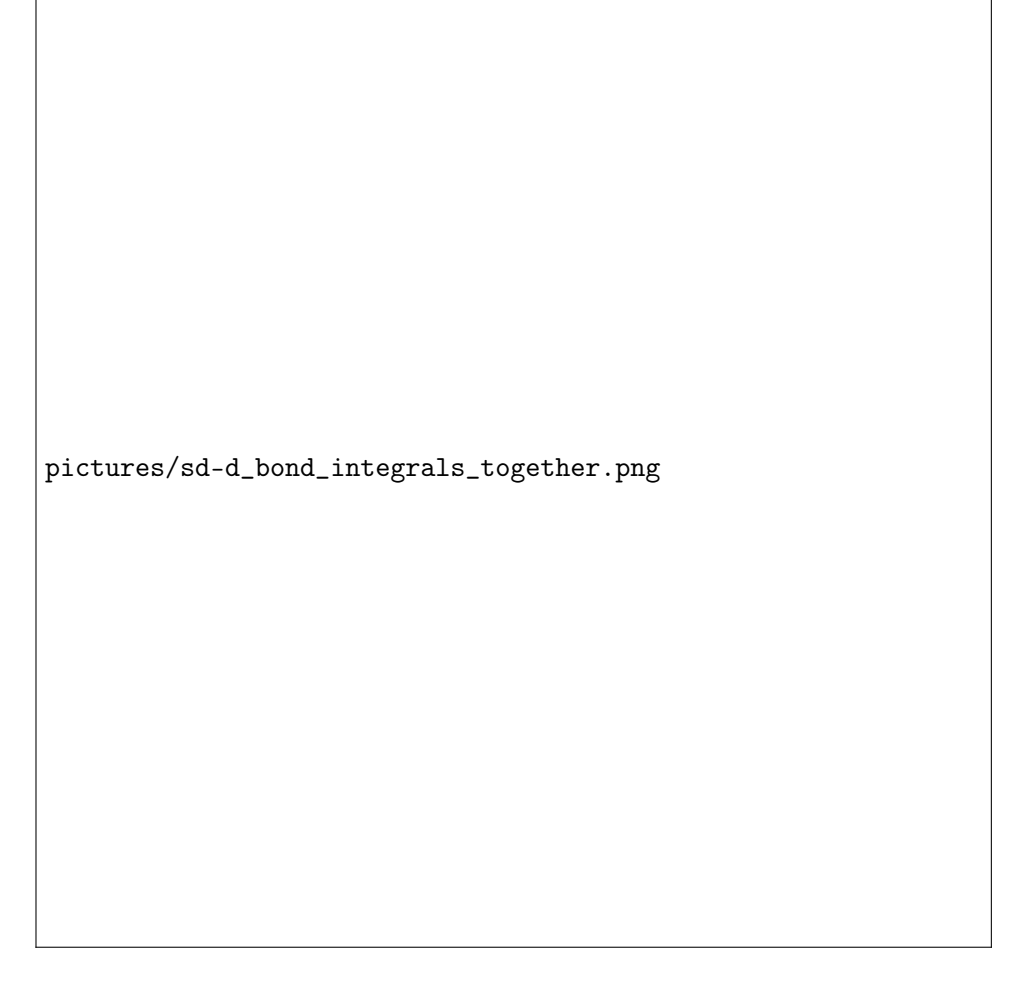
Figure 1: Bond integrals of both d and sd titanium tight-binding models. First and second derivatives shown to demonstrate that there are no abberations when the bond integrals decay to zero between r_1 and r_c.

The bond integrals and pair potential were fitted to reproduce DFT and empirical data, as detailed in table **INSERT TABLE REF**. A loss function was defined as

$$E(\mathbf{x}) = \sum_i w_i(f_i(\mathbf{x}) - \hat{f}_i(\mathbf{x}))^2 + [\alpha||\mathbf{x}||_2 + (1 - \alpha)||\mathbf{x}||_1], \qquad (1)$$

where $\mathbf{x}$ is a vector of input parameters, $f_i(\mathbf{x})$ are quantities calculated from

the input parameters and $\hat{f}_i(\mathbf{x})$ are the respective target quantities from DFT or empirical data. w_i are the weights for each quantity. Quantities of higher importance, such as lattice and elastic constants, were given larger weights in the objective function, as such, the optimiser would have a preference to minimise these quantities. To mitigate the overfitting of parameters (and to dissuade parameters from becoming too large), an Elastic Net regularisation term was added to the loss function, the final term in equation (1), which consists of the L1 and L2 of the input parameter vector $\mathbf{x}$. The L2 norm acts as a penalty for large input parameters, and the L1 norm also gives penalties with the added benefit of allowing sparsity of the parameters: it allows redundant parameters, say in the pair potential, to go to zero [?, ?].

The objective function was minimised within pre-defined constraints by use of the the CMA-ES (Covariance Matrix Adaptation-Evolution Strategy) algorithm by use of the python implementation by Hansen [?]. Parameters put into the CMA-ES algorithm were first transformed to have similar sensitivities with respect to the bounds in which they are sought [?]. This allows for the initial assumption of the CMA-ES algorithm, that the covariance matrix is unity, to be more well satsified, allowing for a more even traversal of the parameter space [?]. Parameters were consequently transformed back, allowing for evaluation of the objective function and loss function, of which the latter was consequently fed into the CMA-ES optimiser.

The data used to fit to was a mix of DFT and empirical data. Great importance was given to the hcp lattice parameter, and the structural energy differences between the titanium polymorphs, all of which were compared to GGA LMTO calculations using the questaal suite [?]. Bandwidths at the high symmetry points of the hcp bands were used as targets, and calculated from DFT by ascertaining bands of dominant d character and taking the difference between the highest and lowest eigenvalues. d character was determined by by decomposition of the eigenvector norm by summation over corresponding orbital subsets, similar to a Mulliken analysis.

To hasten the fitting of parameters, if a set of parameters produced a quantity which was out of an acceptable range, then the objective function would immediately cease and submit a large value to the objective function, dissuading the optimisation algorithm from searching around that area in parameter space.

Results from the first stages of fitting found that soft modes would appear in the phonon spectra for omega and hcp phases. As such it was necessary to calculate the phonon density of states in the objective function, to check that there are no negative densities, as represented in the `phonopy` code [?] .

The parameters obtained are shown in table 1

Quantity	d model	sd model	Target
a_{hcp} []	5.585	5.674	5.577
$c/a(\text{hcp})$	1.584	1.586	1.587
a_{omega} []	8.935	9.039	8.733
c_{omega} []	5.387	5.486	5.323
a_{4h} []	5.576	5.681	5.563
c_{4h} []	18.098	18.328	17.759
a_{6h} []	5.574	5.676	5.546
c_{6h} []	27.184	27.579	26.771
a_{bcc} []	6.201	6.201	6.179
a_{fcc} []	7.873	8.013	7.887
$E(\omega) - E(\text{hcp})$[]	0.588	-0.357	-0.633
$E(4h) - E(\text{hcp})$ []	1.580	1.663	3.172
$E(6h) - E(\text{hcp})$ []	2.483	2.400	3.720
$E(\text{bcc}) - E(\text{hcp})$ []	5.351	7.958	7.635
$E(\text{fcc}) - E(\text{hcp})$ []	3.780	3.825	4.519
C_{11} []	171.6	167.3	176.1
C_{33} []	198.9	205.2	190.5
C_{44} []	47.4	46.6	50.8
C_{12} []	94.7	96.7	86.9
C_{13} []	61.2	60.9	68.3
hcp bandwidth Γ []	3.69	8.90	5.87
hcp bandwidth K []	4.65	4.79	4.97
hcp bandwidth M []	5.19	5.54	7.78
hcp bandwidth L []	4.21	5.43	6.34
hcp bandwidth H []	3.54	4.85	9.70
$E_{\text{prismatic}}$ fault	99.0	110.4	220.0
E_{basal} fault		208.9	
$E_{\text{pyramidal I}}$ fault		154.6	

Table 1: Table of the titanium objective function values compared to DFT target data. The hcp lattice parameter, and the structural energy differences between titanium polymorphs were given large weights in the objective function.

————- $E_{\text{prismaticfault}}$ ————

tbe:	98.953	mJ/m^2
DFT:	250.000	mJ/m^2 [Benoit 2012]
DFT:	233.000	mJ/m^2 [Ackland 1999]

——————- E$_{\text{Basalfault}}$ I2 ——————

$$
\begin{array}{lll}
\text{tbe:} & 211.658 & \text{mJ/m}^2 \\
\text{DFT:} & 260.000 & \text{mJ/m}^2 \quad \text{[Benoit 2012]}
\end{array}
$$

1.3   sd fitting: Including hybridisation

We included s orbitals such that one could more readily model the Ti^{4+} oxidation state of the Ti ion, which would give a more physical representation of titanium ions in quantum electrochemistry calculations.